
Since January 2020 Elsevier has created a COVID-19 resource centre with free information in English and Mandarin on the novel coronavirus COVID-19. The COVID-19 resource centre is hosted on Elsevier Connect, the company's public news and information website.

Virus Research 246 (2018) 28–34

Contents lists available at ScienceDirect

Virus Research

journal homepage: www.elsevier.com/locate/virusres

Short communication

# Antiviral activity of K22 against members of the order Nidovirales

Julie Christiane Françoise Rappe[a,b,c,1], Adriaan de Wilde[d], Han Di[e], Christin Müller[f], Hanspeter Stalder[a,c], Philip V'kovski[a,b,c], Eric Snijder[d], Margo A. Brinton[e], John Ziebuhr[f], Nicolas Ruggli[a,c], Volker Thiel[a,c,*]

[a] Institute for Virology and Immunology IVI, Mittelhäusern and Bern, Switzerland
[b] Graduate School for Cellular and Biomedical Sciences, University of Bern, Switzerland
[c] Department of Infectious Diseases and Pathobiology, University of Bern, Switzerland
[d] Molecular Virology Laboratory, Department of Medical Microbiology, Leiden University Medical Center, Leiden, The Netherlands
[e] Department of Biology, 623 Petit Science Center, Georgia State University, 161 Jesse Hill Jr Drive, Atlanta, GA 30303, United States
[f] Institute of Medical Virology, Justus Liebig University, Giessen, Germany

ARTICLE INFO

*Keywords:*
Nidoviruses
K22
Antiviral drug
Replication organelles
Double membrane vesicles

ABSTRACT

Recently, a novel antiviral compound (K22) that inhibits replication of a broad range of animal and human coronaviruses was reported to interfere with viral RNA synthesis by impairing double-membrane vesicle (DMV) formation (Lundin et al., 2014). Here we assessed potential antiviral activities of K22 against a range of viruses representing two (sub)families of the order *Nidovirales*, the *Arteriviridae* (porcine reproductive and respiratory syndrome virus [PRRSV], equine arteritis virus [EAV] and simian hemorrhagic fever virus [SHFV]), and the *Torovirinae* (equine torovirus [EToV] and White Bream virus [WBV]).

Possible effects of K22 on nidovirus replication were studied in suitable cell lines. K22 concentrations significantly decreasing infectious titres of the viruses included in this study ranged from 25 to 50 μM. Reduction of double-stranded RNA intermediates of viral replication in nidovirus-infected cells treated with K22 confirmed the anti-viral potential of K22. Collectively, the data show that K22 has antiviral activity against diverse lineages of nidoviruses, suggesting that the inhibitor targets a critical and conserved step during nidovirus replication.

The order *Nidovirales* was defined by the International Committee on Taxonomy of Viruses (ICTV) at the X[th] International Congress of Virology in Jerusalem in 1996, and currently includes four virus families: *Arteriviridae*, *Mesoniviridae*, *Roniviridae* and *Coronaviridae*, the latter being divided into the sub-families *Coronavirinae* and *Torovirinae*. Nidoviruses infect diverse host species ranging from mammals to birds, fish, crustaceans and insects (Blanck and Ziebuhr, 2016; Faisal et al., 2016; Wernery et al., 2016; Wickramasinghe et al., 2011; Zeng et al., 2016). Despite considerable diversity in terms of genome size and virion morphology, nidoviruses have been grouped together in the same virus order based on their similar genome organization, a conserved set of domains and enzymatic functions in their replicase polyproteins, and their unique transcription strategy that results in production of a set of nested (Latin *nidus*; nest) subgenomic mRNAs (Gorbalenya et al., 2006).

Nidoviruses share a positive single-stranded, non-segmented, polycistronic genomic RNA that is 3′-polyadenylated and possesses a 5′ cap structure (Nga et al., 2011; Ulferts and Ziebuhr, 2011; Zirkel et al., 2011). Translation of the genomic RNA gives rise to two polyproteins – pp1a and pp1ab, derived from the overlapping open reading frames ORF1a and ORF1a/b, respectively. Synthesis of pp1ab involves a −1 ribosomal frameshift event occurring a few nucleotides upstream the ORF1a stop codon (Firth and Brierley, 2012; Lauber et al., 2013). Pp1a and pp1ab are co- and post-translationally cleaved autoproteolytically to produce the 12–16 non-structural proteins (nsps) that form the

*Abbreviations:* CAVV, Cavally virus; CM, convoluted membrane; DMEM, Dulbecco's modified Eagle's medium; DMSO, dimethyl sulfoxide; DMV, double membrane vesicles; DNA, deoxyribonucleic acid; dsRNA, double-stranded RNA; EAV, equine arteritis virus; EToV, equine torovirus; ER, endoplasmic reticulum; FBS, foetal bovine serum; FCoV, feline coronavirus; HCV, hepatitis C virus; IBV, avian infectious bronchitis virus; ICTV, International Committee for the Taxonomy of Viruses; MERS-CoV, Middle East respiratory syndrome coronavirus; mRNA, messenger RNA; NS5A, non-structural protein 5A; nsp6, non-structural protein 6; ORF, open reading frame; PEDV, porcine epidemic diarrhea virus; PRRSV, porcine reproductive and respiratory syndrome virus; RNA, ribonucleic acid; RTC, replication-transcription complex; RVN, reticulo-vesicular network; SARS-CoV, severe acute respiratory syndrome coronavirus; SHFV, simian haemorrhagic fever virus; TCID, tissue culture infective dose; UTR, untranslated region

* Corresponding author at: Institute for Virology and Immunology IVI, Mittelhäusern and Bern, Switzerland.
*E-mail addresses:* julie.rappe@crick.ac.uk (J.C.F. Rappe), A.H.de_Wilde@lumc.nl (A. de Wilde), hdi1@gsu.edu (H. Di), Christin.Mueller@viro.med.uni-giessen.de (C. Müller), hanspeter.stalder@vetsuisse.unibe.ch (H. Stalder), philip.vkovski@vetsuisse.unibe.ch (P. V'kovski), e.j.snijder@lumc.nl (E. Snijder), mbrinton@gsu.edu (M.A. Brinton), John.Ziebuhr@viro.med.uni-giessen.de (J. Ziebuhr), nicolas.ruggli@ivi.admin.ch (N. Ruggli), volker.thiel@vetsuisse.unibe.ch (V. Thiel).
[1] Current address: Francis Crick Institute, London, United Kingdom, UK.

https://doi.org/10.1016/j.virusres.2018.01.002
Received 8 November 2017; Received in revised form 10 January 2018; Accepted 10 January 2018
Available online 11 January 2018

replication-transcription complex (RTC) (Ziebuhr et al., 2000). Three enzymatic activities encoded in the nidovirus replicase gene are remarkably conserved: a chymotrypsin-like protease (Blanck et al., 2014; Ziebuhr and Siddell, 1999; Ziebuhr et al., 2000), an RNA-dependent RNA polymerase (De Vries et al., 1997; Dennis and Brian, 1981; Koonin, 1991; Lehmann et al., 2016; Nedialkova et al., 2009; Snijder and Meulenberg, 1998) and a superfamily 1 helicase (Lehmann et al., 2015; Seybert et al., 2000; Snijder and Horzinek, 1993).

A hallmark of nidovirus replication, which gave the order its name, is the common transcription strategy that gives rise to a nested set of 3′ co-terminal sub-genomic mRNAs that are translated to produce the structural and accessory proteins (van Vliet et al., 2002). In most nidoviruses (corona-, arteri-, and mesoniviruses), the 5′-terminal part of their subgenomic mRNAs consist of the 5′-terminal segment of the genomic RNA and are therefore regarded as leader sequence (Pasternak et al., 2006; Sawicki et al., 2007; Schutze et al., 2006; van Marle et al., 1999; Zirkel et al., 2013). However, for the toroviruses, only the largest subgenomic mRNA has a 5′ leader sequence (Smits et al., 2005) while the smaller subgenomic mRNAs do not contain a leader sequence. No common leader sequence has been identified for roniviral subgenomic mRNAs (Cowley et al., 2002). The current model of nidovirus transcription is a nested set of negative-stranded RNAs of subgenomic-length produced by using the genomic RNA as template and specific transcription-regulatory sequences (TRSs) to attenuate negative strand RNA synthesis at these specific sites (Pasternak et al., 2006; Sawicki et al., 2007). The subgenomic negative-strand RNAs templates the synthesis of subgenomic mRNAs.

Positive-stranded RNA viruses are known to induce the formation of replication organelles consisting of modified intracellular host membranes associated with replicative enzyme complexes. These specialized microenvironments are presumed to facilitate the assembly and function of the viral RNA-synthesizing machinery, and may also function to delay or prevent the detection of double-stranded RNA (dsRNA) intermediates of viral replication by innate immune sensors (Ahlquist et al., 2003; Angelini et al., 2014; den Boon and Ahlquist, 2010; Neufeldt et al., 2016; Salonen et al., 2005; Schwartz et al., 2004). Following the emergence of new three-dimensional imaging techniques, such as electron cryo-tomography, the ultrastructural organization of these host-derived replication organelles have been intensively studied for a number of positive-strand RNA viruses including coronaviruses, toroviruses and arteriviruses (Avila-Perez et al., 2016; Knoops et al., 2012; Knoops et al., 2008; Maier et al., 2013; Romero-Brey and Bartenschlager, 2015; van der Hoeven et al., 2016). Coronavirus replication occurs within the cytoplasm of infected cells where mainly endoplasmic reticulum (ER) membranes appear to be recruited for the formation of replication organelles. This results in the formation of a reticulo-vesicular network (RVN) that is continuous with the ER and includes double-membrane vesicles (DMV) and convoluted membranes (CM) (de Wilde et al., 2013b; Gosert et al., 2002; Knoops et al., 2008; Orenstein et al., 2008). Additionally, Avian infectious bronchitis virus (IBV) was reported induce invaginated structures, identified as zippered endoplasmic reticulum and double-membrane spherules (Maier et al., 2013). The arterivirus prototype equine arteritis virus (EAV) induces DMVs similar to those of coronaviruses, whose outer membranes are interconnected with each other and with the ER, thus forming a RVN (Knoops et al., 2012). Similar virus-induced membrane re-arrangements were also described for other arteriviruses including porcine reproductive and respiratory syndrome virus (PRRSV) and simian hemorrhagic fever virus (SHFV) (Metwally et al., 2010; Sun et al., 2012; Wood et al., 1970). The host-derived membrane structures induced by a torovirus infection were described for the first time in a recent study (Avila-Perez et al., 2016). Using cells infected with the equine torovirus (EToV) prototype, Avila-Pérez and colleagues described the presence of DMVs of heterogeneous size in the cytoplasm of infected cells, located frequently in the perinuclear area and surrounded by mitochondria and ER membranes. Unlike coronaviruses infected cells, no CM or spherules were identified. For the nidoviruses mentioned above (corona-, arteri- and toroviruses), the use of confocal and transmission electron microscopy showed the association of key replicative enzymes of the replication transcription complex (RTC) with the modified host membrane structures (Pedersen et al., 1999; Posthuma et al., 2008; Snijder et al., 2006; van Hemert et al., 2008) and the accumulation of double-stranded RNA in the DMV interior (Avila-Perez et al., 2016; Knoops et al., 2012; Knoops et al., 2008).

The first insect nidoviruses were isolated in Vietnam in 2001–2003 and Côte d'Ivoire in 2009, during surveillance studies of virus infection rates in mosquitoes (Junglen et al., 2009; Nga et al., 2011). The Ivorian isolate, Cavally virus (CavV), is the prototype of the newly established nidovirus family *Mesoniviridae* (Zirkel et al., 2011). Details of the mesonivirus life cycle, however, have not yet been thoroughly studied, including the question of whether or not similar host membrane structures are involved in mesonivirus replication (Vasilakis et al., 2014).

The striking conservation of the nidoviral strategies for RNA synthesis and gene expression suggests that inhibitors targeting common mechanisms of the nidovirus replication cycle may have broad "anti-nidovirus" activity. Indeed, cyclophilin inhibitor was found to affect the replication of diverse coronaviruses and arteriviruses including MERS-CoV, SARS-CoV, human coronavirus 229E, feline coronavirus (FCoV), mouse hepatitis virus (MHV), EAV and PRRSV in cell culture (de Wilde et al., 2013a; de Wilde et al., 2013b; de Wilde et al., 2011; Pfefferle et al., 2011; Tanaka et al., 2012). More recently, an antiviral compound − K22, whose structural name is (*Z*)-*N*-(3-(4-(4-bromophenyl)-4-hydroxypiperidin-1-yl)-3-oxo-1-phenylprop-1-en-2-yl) benzamide − was demonstrated to inhibit the replication of six different coronaviruses in cell culture (Lundin et al., 2014). Electron microscopic analyses and the observation that K22-resistance can be due to mutations in nsp6 (a membrane-spanning non-structural protein that is an integral component of the coronavirus replication complex implicated in DMV formation) suggest that the antiviral effect of K22 is linked to the inhibition of membrane-bound coronaviruses RNA synthesis.

Considering the similarities in genome organization and expression, RNA replication and transcription, and the membrane structures involved in RNA synthesis among viruses of the *Nidovirales* order, we investigated whether K22 similarly inhibits the replication of nidoviruses beyond the *Coronaviridae* subfamily, *i.e.* the arteri-, toro-, bafini-, and mesoniviruses.

Due to the close phylogenetic relationship to coronaviruses, we assessed potential anti-viral effects of K22 of two members of the coronavirus subfamily *Torovirinae*, namely the equine torovirus (EToV; genus *Torovirus*) and the white bream virus (WBV; genus *Bafinivirus*). Horse dermal fibroblast cells (NBL-6, also known as E-Derm) were infected with EToV (strain Berne virus) at a multiplicity of infection (MOI) of 0.001. Four hours prior to infection, cells were treated with different K22 concentrations or the solvent (DMSO) as a control. Two days post infection, EToV infectivity titres in the supernatant were determined by end-point dilution on E-Derm cells and expressed as $TCID_{50}$/ml calculated using the Reed-Muench formula (Reed and Muench, 1938). As shown in Fig. 1A, treatment of E-Derm cells with 40 μM of K22 resulted in significantly reduced EToV titres (3.5 $\log_{10}$) compared with titres obtained on cells treated with DMSO. Importantly, E-Derm viability measured with a Promega CytoTox-Glo™ Cytotoxicity Assay in the presence of K22 did not show any cytotoxic effect at the concentrations used in our experiments, suggesting that K22 exerts antiviral activity against EToV (Fig. 1A). We also assessed the effect of K22 on fish EPC cells (*Epithelioma Papulosum Cyprini*) infected with the bafinivirus WBV. Viral RNA levels in cells were measured by quantitative PCR at 12 h post infection. As shown in Fig. 1B, WBV replication was significantly reduced in a dose-dependent manner. At the highest K22 concentration used (50 μM), we observed a reduction of 1.6 $\log_{10}$ WBV genome equivalents (GE)/ml while the viability of EPC cells

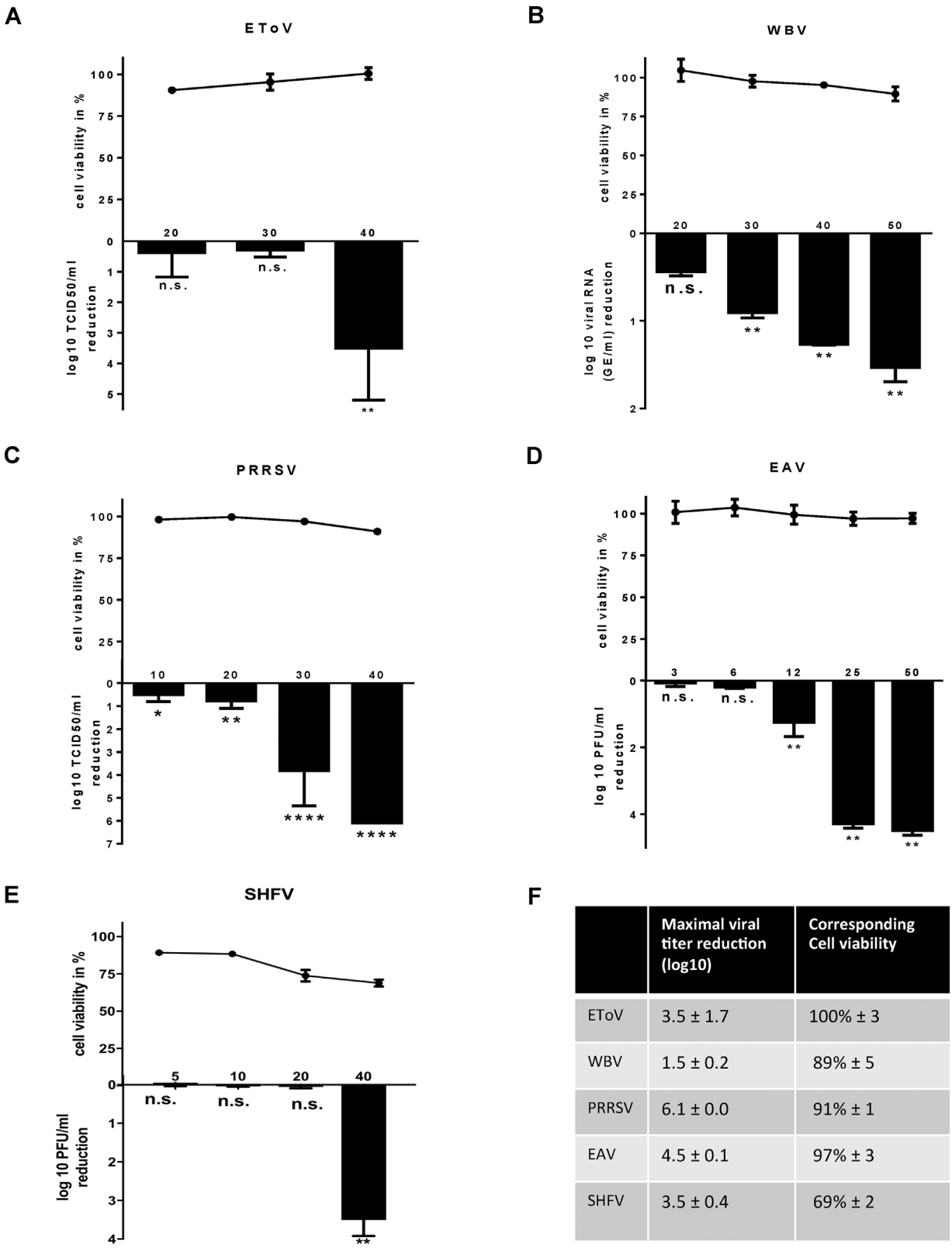


F

| | Maximal viral titer reduction (log10) | Corresponding Cell viability |
|---|---|---|
| EToV | 3.5 ± 1.7 | 100% ± 3 |
| WBV | 1.5 ± 0.2 | 89% ± 5 |
| PRRSV | 6.1 ± 0.0 | 91% ± 1 |
| EAV | 4.5 ± 0.1 | 97% ± 3 |
| SHFV | 3.5 ± 0.4 | 69% ± 2 |

**Fig. 1.** K22 affects diverse nidoviruses.

The log reduction in virus yield (bars) and the percent of cell viability (solid line above bars) are shown for K22-treated torovirus- (A) bafinivirus- (B) and arterivirus-infected (C, D and E) cell lines of equine (E-Derm for EToV), fish (EPC for WBV), primate (MARC-145 for PRRSV and MA-104 cells for SHFV) or rodent (BHK-21 for EAV) origin. The cells were infected 4 h after treatment with different concentrations of K22 or solvent (DMSO) as a control. At 12 h (WBV, EAV), 24 h (SHFV) or 48 h (EtoV, PRRSV) post infection, viral titres or intracellular RNA levels were determined. Log reduction of virus production induced by K22 was calculated by comparing titres obtained in DMSO-treated cells (control) with titres obtained in cells treated with different concentrations of K22. Cytotoxicity was assessed with a Promega CytoTox-Glo™ Cytotoxicity Assay (for EToV), a CellTiter 96 $AQ_{ueous}$ nonradioactive cell proliferation assay (for PRRSV and EAV) or a MTT assay (for SHFV and WBV) and expressed in% of cell viability. Maximal viral titre reduction and the associated cell viability were determined for each virus and summarized in table format (F). Data are shown as mean ( ± SD) of 3–9 biological repeats. Statistical test: Mann-Whitney. n.s. = non-significant, *: $p < 0.1$, **: $p < 0.01$, ***: $p < 0.001$, ****: $p < 0.0001$.

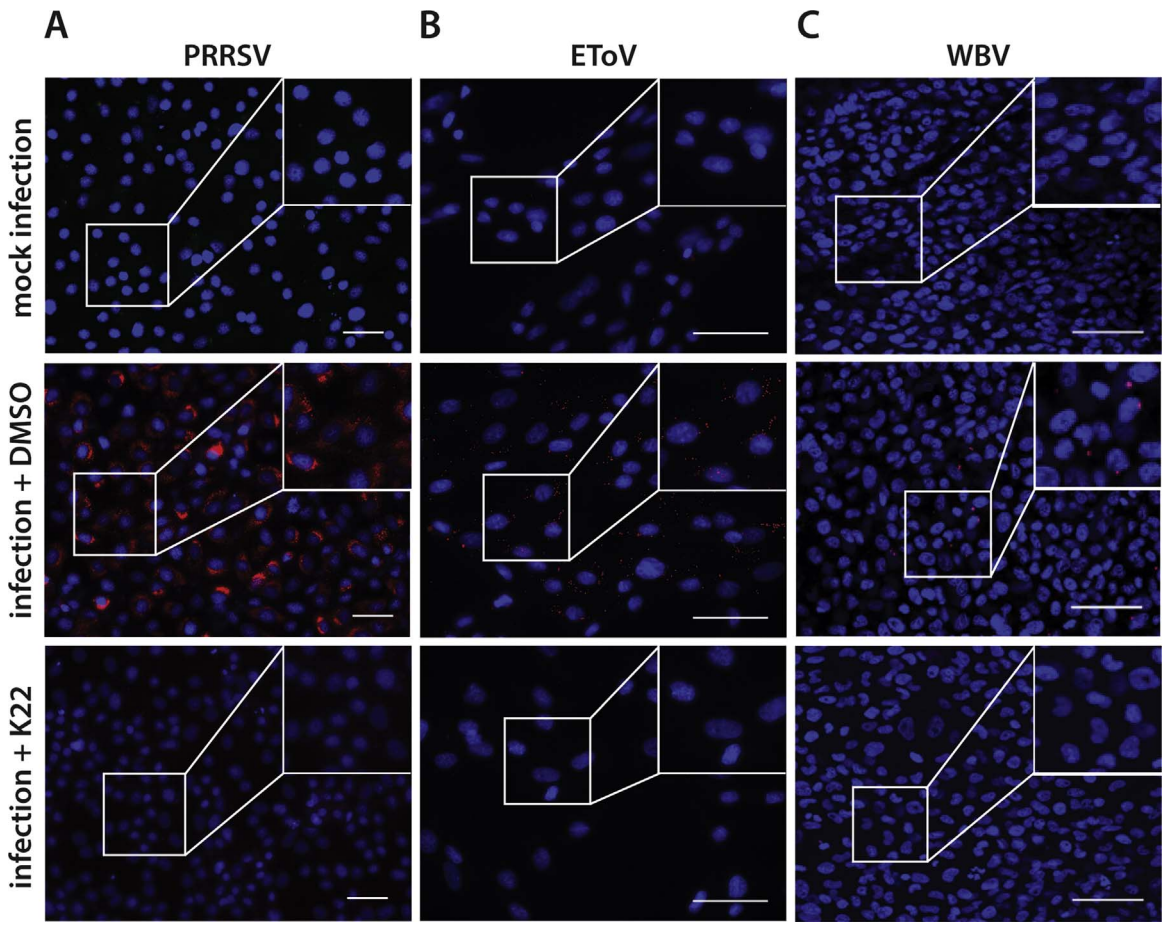


**Fig. 2.** Impact of K22 on dsRNA accumulation during nidovirus infection.
MARC-145 (A), E-Derm (B) and EPC (C) cells were infected with an arterivirus (PRRSV), a torovirus (EToV) and a bafinivirus (WBV), respectively and incubated for 12 h (C), 16 h (B) or 24 h (A) in the presence of 40 μM of K22 or DMSO. The cells were then fixed with 4% paraformaldehyde and processed for immunofluorescence staining with monoclonal anti-dsRNA J2 antibody (in red) and DAPI (cell nucleus in blue). Scale bar is 50 μm.

remained around 90%.

We next expanded our investigation to the arteriviruses. MARC-145, BHK-21 and MA-104 cells were infected with PRRSV (genotype 2, strain RVB-581, MOI of 0.5), EAV (strain Bucyrus, MOI of 5) and SHFV (strain LVR 42-0/M6941, MOI of 1), respectively, 4 h after treatment with different concentrations of K22. PRRSV titres in the supernatant were measured by end-point dilution at 48 h post infection and expressed as $TCID_{50}$/ml calculated using the Reed-Muench formula whereas EAV and SHFV titres in the supernatant at 12 h and 24 h post infection, respectively, were measured by plaque assays and expressed in PFU/ml. As shown in Fig. 1C–E, PRRSV, EAV, and SHFV titres were reduced in a dose-dependent manner by K22 treatment, with a maximal titre reduction of 6.1 $\log_{10}$ (PRRSV), 4.5 $\mathrm{Log}_{10}$ (EAV) and 3.5 $\log_{10}$ (SHFV), respectively. Notably, at the highest K22 concentration used for PRRSV inhibition (40 μM), infectious PRRSV was no longer detectable in cell culture supernatants. Concerning the reduction of SHFV replication (Fig. 1E), we observed reduced cell viability of MA-104 cells measured using an MTT assay at K22 concentrations of 20 and 40 μM, suggesting that the observed 3.5 $\log_{10}$ reduction of SHFV replication may be overestimated. In fact, since we did not observe reduction of SHFV replication in a dose-dependent manner, we consider that K22 may actually not, or only marginally, impact on SHFV replication. Importantly, however, we did not observe any K22-related cytotoxicity in MARC-145 and BHK-21 cells, using a CellTiter 96 $AQ_{ueous}$ non-radioactive cell proliferation assay (Promega), a colorimetric method for determining the number of viable cells in proliferation. This demonstrates that K22 is highly active in inhibiting PRRSV and EAV replication (Fig. 1C, D).

Finally, we analysed whether K22 displays antiviral activity against Cavally virus (CavV; family *Mesoniviridae*). CavV is an invertebrate nidovirus infecting insects (mosquitoes) and C6/36 mosquito cells have been used to propagate this virus *in vitro*. However, since we observed considerable reduction in viability of K22-treated C6/36 cells, it was not possible to assess any selective antiviral activity of K22 against CavV (data not shown).

In order to confirm the effect of K22 on nidovirus replication, we monitored the accumulation of double-stranded RNA (dsRNA) – intermediates of viral RNA synthesis widely used as marker of positive RNA virus replication – in infected cells by immunofluorescence microscopy. MARC-145, E-Derm and EPC cells were treated with 40 μM of K22 or DMSO and infected simultaneously with PRRSV (Fig. 2A), EToV (Fig. 2B) and WBV (Fig. 2C), respectively. At 12–24 h post infection, the cells were fixed and stained with anti-dsRNA monoclonal antibody J2 (English & Scientific Consulting Bt). As shown in Fig. 2, dsRNA was readily detectable as a perinuclear punctate pattern in PRRSV-, EToV-, and WBV-infected cells treated with the solvent control. In contrast, dsRNA was not, or only barely detectable in infected cells treated with K22, corroborating the observed reduction of virus titres in the supernatants of infected cells (Fig. 1).

K22 was initially identified by screening the ChemBioNet collection of 16671 compounds for anti-HCoV-229E activity. Subsequent analyses revealed that K22 displayed potent inhibition against diverse human and animal coronaviruses. Here we demonstrate that K22 also displays antiviral activity beyond the *Coronavirinae* subfamily, namely against nidoviruses of the *Torovirinae* subfamily (EToV and WBV) and members of the *Arteriviridae* family (PRRSV, EAV, and possibly also SHFV)

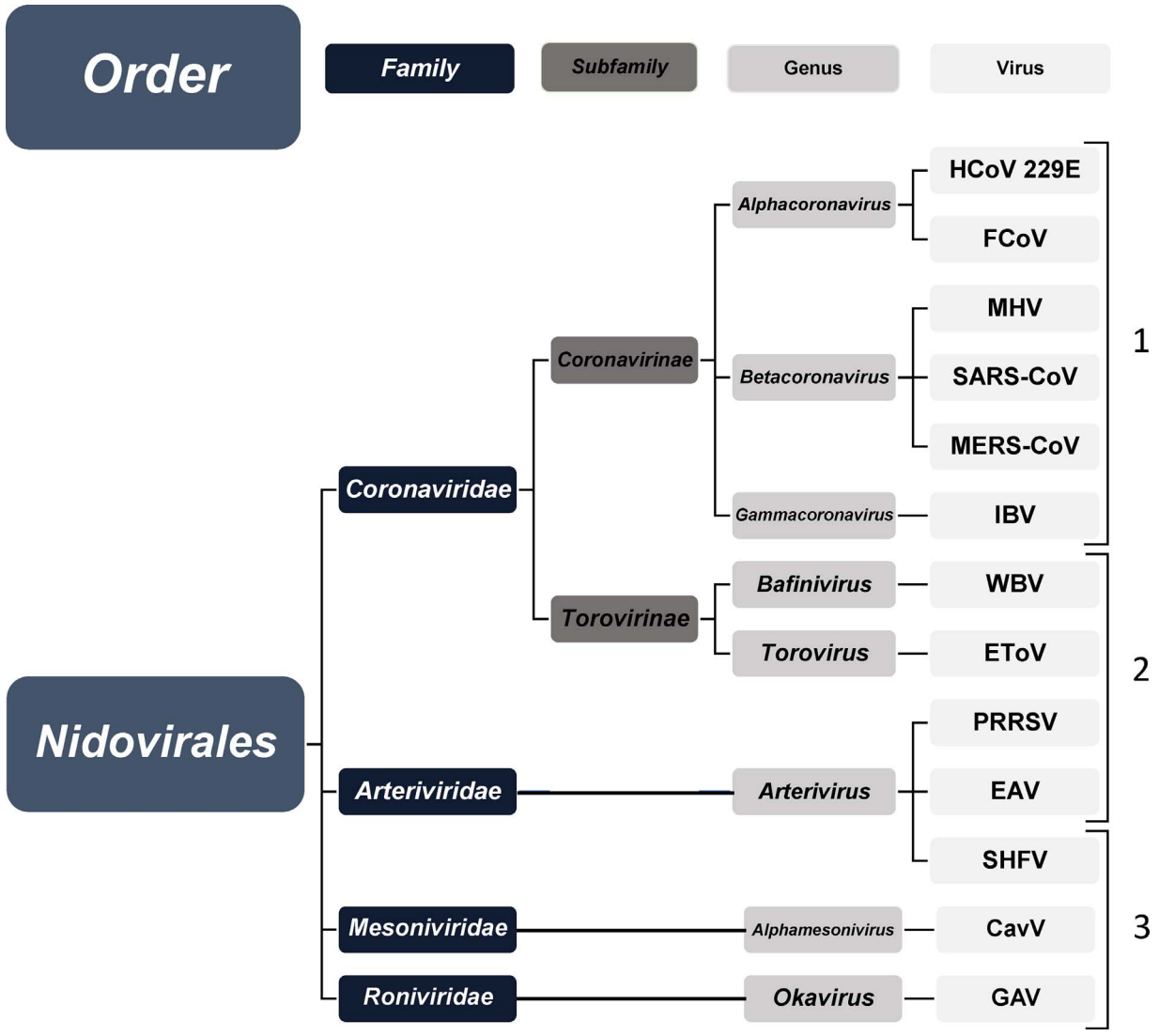


**Fig. 3.** Overview of confirmed antiviral activity of K22 among Nidovirales members. Members of the Nidovirales order confirmed to be affected by K22 according to the present study (2), by Lundin and co-workers (Lundin et al., 2014) (1), as well as nidoviruses that have not yet been shown to be affected by K22 (3) are highlighted in this organigram.

(Fig. 3). As reported previously for diverse coronaviruses (Lundin et al., 2014), the concentrations of K22 required for efficient inhibition of replication varied depending on which virus used. Since the initial screen was performed with HCoV-229E, K22 is most effective against HCoV-229E, and for other nidoviruses higher concentrations are required. In this context it is important to note that there's no indication that at higher concentrations of K22 the cells were not able to process and transport molecules, e.g. as it would be necessary for virus assembly and release. This assumption is further reinforced considering that K22 (up to 40 μM) has no or little effects on Poliovirus replication (Lundin et al., 2014).

The wide anti-viral activity of K22 against nidoviruses suggests similar replicative functions among the members of this order. Whether K22 targets viral or cellular factors, either directly or indirectly, remains to be determined and is currently being addressed in our laboratory. The mechanism of action of K22 has been partially solved for the human coronavirus HCoV-229E (Lundin et al., 2014). Time-of-addition experiments showed that K22 exhibits potent antiviral activity when added up to 6 h for coronaviruses (Lundin et al., 2014) and 8 h for PRRSV (data not shown) after infection of cells, suggesting that K22 was acting at early stages of the post-entry phase. More specifically, the combination of electron and immunofluorescence microscopy techniques suggested that K22 reduces viral replication by targeting replication organelle formation. The selection of escape mutants resistant to K22 by serial passages under increasing K22 concentrations revealed that K22-resistant HCoV-229E mutants carried mutations in nsp6. Unlike parental wild-type HCoV-229E, resistant viral mutants were able to form DMVs and efficiently replicate, even in the presence of K22. The Coronavirus nsp6 protein has multiple membrane-spanning domains (Baliji et al., 2009) and has been implicated in the induction of host cell membrane rearrangements that support coronavirus membrane-bound RNA synthesis. Importantly, expression of nsp6 together with nsp3 and nsp4, induces double-membrane vesicles resembling those observed in coronavirus-infected cells (Angelini et al., 2013; Hagemeijer et al., 2014). We speculate that K22 targets a specific virus-host interaction required for virus-induced rearrangement of host membranes. The wide range of K22 antiviral activity against diverse nidoviruses – in cell lines originating from a variety of different host species – suggests that the target of K22 is highly conserved and affects a key step in the nidovirus life cycle. The elucidation of the cellular or viral target of K22 will eventually reveal mechanistic insight about the exact mode of action of K22 and will enhance the development of drugs that target this vulnerable step of nidovirus replication.

## Acknowledgements

The work of JCFR, PV, NR and VT was funded by the Swiss Federal Food Safety and Veterinary Office (FSVO, BLV grant number 1.13.12) and the Swiss National Science Foundation (project number: 149784 and 173085). The work of HD and MAB was supported by a Molecular Basis of Disease seed grant from Georgia State University. The work of CM and JZ was supported by the German Center for Infection Research (DZIF, TTU Emerging Infections). We thank also Ettore Ullo, and Ulrike Claudia Wend for excellent technical assistance.

## References

Ahlquist, P., Noueiry, A.O., Lee, W.M., Kushner, D.B., Dye, B.T., 2003. Host factors in positive-strand RNA virus genome replication. J. Virol. 77 (15), 8181–8186.

Angelini, M.M., Akhlaghpour, M., Neuman, B.W., Buchmeier, M.J., 2013. Severe acute respiratory syndrome coronavirus nonstructural proteins 3, 4, and 6 induce double-membrane vesicles. mBio 4 (4). http://dx.doi.org/10.1128/mBio.00524-13.

Angelini, M.M., Neuman, B.W., Buchmeier, M.J., 2014. Untangling membrane rearrangement in the nidovirales. DNA Cell Biol. 33 (3), 122–127.

Avila-Perez, G., Rejas, M.T., Rodriguez, D., 2016. Ultrastructural characterization of membranous torovirus replication factories. Cell. Microbiol. 8 (12), 1691–1708.

Baliji, S., Cammer, S.A., Sobral, B., Baker, S.C., 2009. Detection of nonstructural protein 6 in murine coronavirus-infected cells and analysis of the transmembrane topology by using bioinformatics and molecular approaches. J. Virol. 83 (13), 6957–6962.

Blanck, S., Ziebuhr, J., 2016. Proteolytic processing of mesonivirus replicase polyproteins by the viral 3C-like protease. J. Gen. Virol. 97 (6), 1439–1445.

Blanck, S., Stinn, A., Tsiklauri, L., Zirkel, F., Junglen, S., Ziebuhr, J., 2014. Characterization of an alphamesonivirus 3C-like protease defines a special group of nidovirus main proteases. J. Virol. 88 (23), 13747–13758.

Cowley, J.A., Dimmock, C.M., Walker, P.J., 2002. Gill-associated nidovirus of Penaeus monodon prawns transcribes 3'-coterminal subgenomic mRNAs that do not possess 5'-leader sequences. J. Gen. Virol. 83 (Pt 4), 927–935.

De Vries, A.A., Horzinek, M.C., Rottier, P.J., De Groot, R.J., 1997. The genome organization of the Nidovirales: similarities and differences between arteri- toro-, and coronaviruses. Semin. Virol. 8, 33–47.

Dennis, D.E., Brian, D.A., 1981. Coronavirus cell-associated RNA-dependent RNA polymerase. Adv. Exp. Med. Biol. 142, 155–170.

de Wilde, A.H., Zevenhoven-Dobbe, J.C., van der Meer, Y., Thiel, V., Narayanan, K., Makino, S., Snijder, E.J., van Hemert, M.J., 2011. Cyclosporin A inhibits the replication of diverse coronaviruses. J. Gen. Virol. 92 (Pt 11), 2542–2548.

de Wilde, A.H., Li, Y., van der Meer, Y., Vuagniaux, G., Lysek, R., Fang, Y., Snijder, E.J., van Hemert, M.J., 2013a. Cyclophilin inhibitors block arterivirus replication by interfering with viral RNA synthesis. J. Virol. 87 (3), 1454–1464.

de Wilde, A.H., Raj, V.S., Oudshoorn, D., Bestebroer, T.M., van Nieuwkoop, S., Limpens, R.W., Posthuma, C.C., van der Meer, Y., Barcena, M., Haagmans, B.L., Snijder, E.J., van den Hoogen, B.G., 2013b. MERS-coronavirus replication induces severe in vitro cytopathology and is strongly inhibited by cyclosporin A or interferon-alpha treatment. J. Gen. Virol. 94 (Pt 8), 1749–1760.

den Boon, J.A., Ahlquist, P., 2010. Organelle-like membrane compartmentalization of positive-strand RNA virus replication factories. Annu. Rev. Microbiol. 64, 241–256.

Faisal, M., Baird, A., Winters, A.D., Millard, E.V., Marcquenski, S., Hsu, H.M., Hennings, A., Bochsler, P., Standish, I., Loch, T.P., Gunn, M.R., Warg, J., 2016. Isolation of the fathead minnow nidovirus from muskellunge experiencing lingering mortality. J. Aquat. Anim. Health 28 (2), 131–141.

Firth, A.E., Brierley, I., 2012. Non-canonical translation in RNA viruses. J. Gen. Virol. 93 (Pt 7), 1385–1409.

Gorbalenya, A.E., Enjuanes, L., Ziebuhr, J., Snijder, E.J., 2006. Nidovirales: evolving the largest RNA virus genome. Virus Res. 117 (1), 17–37.

Gosert, R., Kanjanahaluethai, A., Egger, D., Bienz, K., Baker, S.C., 2002. RNA replication of mouse hepatitis virus takes place at double-membrane vesicles. J. Virol. 76 (8), 3697–3708.

Hagemeijer, M.C., Monastyrska, I., Griffith, J., van der Sluijs, P., Voortman, J., van Bergen en Henegouwen, P.M., Vonk, A.M., Rottier, P.J., Reggiori, F., de Haan, C.A., 2014. Membrane rearrangements mediated by coronavirus nonstructural proteins 3 and 4. Virology 458–459, 125–135.

Junglen, S., Kurth, A., Kuehl, H., Quan, P.L., Ellerbrok, H., Pauli, G., Nitsche, A., Nunn, C., Rich, S.M., Lipkin, W.I., Briese, T., Leendertz, F.H., 2009. Examining landscape factors influencing relative distribution of mosquito genera and frequency of virus infection. EcoHealth 6 (2), 239–249.

Knoops, K., Kikkert, M., Worm, S.H., Zevenhoven-Dobbe, J.C., van der Meer, Y., Koster, A.J., Mommaas, A.M., Snijder, E.J., 2008. SARS-coronavirus replication is supported by a reticulovesicular network of modified endoplasmic reticulum. PLoS Biol. 6 (9), e226. http://dx.doi.org/10.1371/journal.pbio.0060226.

Knoops, K., Barcena, M., Limpens, R.W., Koster, A.J., Mommaas, A.M., Snijder, E.J., 2012. Ultrastructural characterization of arterivirus replication structures: reshaping the endoplasmic reticulum to accommodate viral RNA synthesis. J. Virol. 86 (5), 2474–2487.

Koonin, E.V., 1991. The phylogeny of RNA-dependent RNA polymerases of positive-strand RNA viruses. J. Gen. Virol. 72 (Pt 9), 2197–2206.

Lauber, C., Goeman, J.J., Parquet Mdel, C., Nga, P.T., Snijder, E.J., Morita, K., Gorbalenya, A.E., 2013. The footprint of genome architecture in the largest genome expansion in RNA viruses. PLoS Pathog. 9 (7), e1003500. http://dx.doi.org/10.1371/journal.ppat.1003500.

Lehmann, K.C., Snijder, E.J., Posthuma, C.C., Gorbalenya, A.E., 2015. What we know but do not understand about nidovirus helicases. Virus Res. 202, 12–32.

Lehmann, K.C., Gorbalenya, A.E., Snijder, E.J., Posthuma, C.C., 2016. Arterivirus RNA-dependent RNA polymerase: vital enzymatic activity remains elusive. Virology 487, 68–74.

Lundin, A., Dijkman, R., Bergstrom, T., Kann, N., Adamiak, B., Hannoun, C., Kindler, E., Jonsdottir, H.R., Muth, D., Kint, J., Forlenza, M., Muller, M.A., Drosten, C., Thiel, V., Trybala, E., 2014. Targeting membrane-bound viral RNA synthesis reveals potent inhibition of diverse coronaviruses including the middle East respiratory syndrome virus. PLoS Pathog. 10 (5), e1004166. http://dx.doi.org/10.1371/journal.ppat.1004166.

Maier, H.J., Hawes, P.C., Cottam, E.M., Mantell, J., Verkade, P., Monaghan, P., Wileman, T., Britton, P., 2013. Infectious bronchitis virus generates spherules from zippered endoplasmic reticulum membranes. mBio 4 (5), e00801–e00813. http://dx.doi.org/10.1128/mBio.00801-13.

Metwally, S., Mohamed, F., Faaberg, K., Burrage, T., Prarat, M., Moran, K., Bracht, A., Mayr, G., Berninger, M., Koster, L., To, T.L., Nguyen, V.L., Reising, M., Landgraf, J., Cox, L., Lubroth, J., Carrillo, C., 2010. Pathogenicity and molecular characterization of emerging porcine reproductive and respiratory syndrome virus in Vietnam in 2007. Transbound. Emerg. Dis. 57 (5), 315–329.

Nedialkova, D.D., Ulferts, R., van den Born, E., Lauber, C., Gorbalenya, A.E., Ziebuhr, J., Snijder, E.J., 2009. Biochemical characterization of arterivirus nonstructural protein 11 reveals the nidovirus-wide conservation of a replicative endoribonuclease. J. Virol. 83 (11), 5671–5682.

Neufeldt, C.J., Joyce, M.A., Van Buuren, N., Levin, A., Kirkegaard, K., Gale Jr., M., Tyrrell, D.L., Wozniak, R.W., 2016. The hepatitis C virus-induced membranous web and associated nuclear transport machinery limit access of pattern recognition receptors to viral replication sites. PLoS Pathog. 12 (2), e1005428. http://dx.doi.org/10.1371/journal.ppat.1005428.

Nga, P.T., Parquet Mdel, C., Lauber, C., Parida, M., Nabeshima, T., Yu, F., Thuy, N.T., Inoue, S., Ito, T., Okamoto, K., Ichinose, A., Snijder, E.J., Morita, K., Gorbalenya, A.E., 2011. Discovery of the first insect nidovirus, a missing evolutionary link in the emergence of the largest RNA virus genomes. PLoS Pathog. 7 (9), e1002215. http://dx.doi.org/10.1371/journal.ppat.1002215.

Orenstein, J.M., Banach, B., Baker, S.C., 2008. Morphogenesis of coronavirus HCoV-NL63 in cell culture: a transmission electron microscopic study. Open Infect. Dis. J. 2, 52–58.

Pasternak, A.O., Spaan, W.J., Snijder, E.J., 2006. Nidovirus transcription: how to make sense…? J. Gen. Virol. 87 (Pt 6), 1403–1421.

Pedersen, K.W., van der Meer, Y., Roos, N., Snijder, E.J., 1999. Open reading frame 1a-encoded subunits of the arterivirus replicase induce endoplasmic reticulum-derived double-membrane vesicles which carry the viral replication complex. J. Virol. 73 (3), 2016–2026.

Pfefferle, S., Schopf, J., Kogl, M., Friedel, C.C., Muller, M.A., Carbajo-Lozoya, J., Stellberger, T., von Dall'Armi, E., Herzog, P., Kallies, S., Niemeyer, D., Ditt, V., Kuri, T., Zust, R., Pumpor, K., Hilgenfeld, R., Schwarz, F., Zimmer, R., Steffen, I., Weber, F., Thiel, V., Herrler, G., Thiel, H.J., Schwegmann-Wessels, C., Pohlmann, S., Haas, J., Drosten, C., von Brunn, A., 2011. The SARS-coronavirus-host interactome: identification of cyclophilins as target for pan-coronavirus inhibitors. PLoS Pathog. 7 (10), e1002331. http://dx.doi.org/10.1371/journal.ppat.1002331.

Posthuma, C.C., Pedersen, K.W., Lu, Z., Joosten, R.G., Roos, N., Zevenhoven-Dobbe, J.C., Snijder, E.J., 2008. Formation of the arterivirus replication/transcription complex: a key role for nonstructural protein 3 in the remodeling of intracellular membranes. J. Virol. 82 (9), 4480–4491.

Reed, L.J., Muench, H., 1938. A simple method of estimating fifty per cent endpoints 1 2. Am. J. Epidemiol. 27 (3), 493–497.

Romero-Brey, I., Bartenschlager, R., 2015. Viral infection at high magnification: 3D electron microscopy methods to analyze the architecture of infected cells. Viruses 7 (12), 6316–6345.

Salonen, A., Ahola, T., Kaariainen, L., 2005. Viral RNA replication in association with cellular membranes. Curr. Top. Microbiol. Immunol. 285, 139–173.

Sawicki, S.G., Sawicki, D.L., Siddell, S.G., 2007. A contemporary view of coronavirus transcription. J. Virol. 81 (1), 20–29.

Schutze, H., Ulferts, R., Schelle, B., Bayer, S., Granzow, H., Hoffmann, B., Mettenleiter, T.C., Ziebuhr, J., 2006. Characterization of White bream virus reveals a novel genetic cluster of nidoviruses. J. Virol. 80 (23), 11598–11609.

Schwartz, M., Chen, J., Lee, W.M., Janda, M., Ahlquist, P., 2004. Alternate, virus-induced membrane rearrangements support positive-strand RNA virus genome replication. Proc. Natl. Acad. Sci. U. S. A. 101 (31), 11263–11268.

Seybert, A., van Dinten, L.C., Snijder, E.J., Ziebuhr, J., 2000. Biochemical characterization of the equine arteritis virus helicase suggests a close functional relationship between arterivirus and coronavirus helicases. J. Virol. 74 (20), 9586–9593.

Smits, S.L., van Vliet, A.L., Segeren, K., el Azzouzi, H., van Essen, M., de Groot, R.J., 2005. Torovirus non-discontinuous transcription: mutational analysis of a subgenomic mRNA promoter. J. Virol. 79 (13), 8275–8281.

Snijder, E.J., Horzinek, M.C., 1993. Toroviruses: replication, evolution and comparison with other members of the coronavirus-like superfamily. J. Gen. Virol. 74 (Pt 11), 2305–2316.

Snijder, E.J., Meulenberg, J.J., 1998. The molecular biology of arteriviruses. J. Gen. Virol. 79 (Pt 5), 961–979.

Snijder, E.J., van der Meer, Y., Zevenhoven-Dobbe, J., Onderwater, J.J., van der Meulen, J., Koerten, H.K., Mommaas, A.M., 2006. Ultrastructure and origin of membrane vesicles associated with the severe acute respiratory syndrome coronavirus replication complex. J. Virol. 80 (12), 5927–5940.

Sun, M.X., Huang, L., Wang, R., Yu, Y.L., Li, C., Li, P.P., Hu, X.C., Hao, H.P., Ishag, H.A., Mao, X., 2012. Porcine reproductive and respiratory syndrome virus induces autophagy to promote virus replication. Autophagy 8 (10), 1434–1447.

Tanaka, Y., Sato, Y., Osawa, S., Inoue, M., Tanaka, S., Sasaki, T., 2012. Suppression of feline coronavirus replication in vitro by cyclosporin A. Vet. Res. 43, 41.

Ulferts, R., Ziebuhr, J., 2011. Nidovirus ribonucleases: structures and functions in viral replication. RNA Biol. 8 (2), 295–304.

van Hemert, M.J., van den Worm, S.H., Knoops, K., Mommaas, A.M., Gorbalenya, A.E., Snijder, E.J., 2008. SARS-coronavirus replication/transcription complexes are membrane-protected and need a host factor for activity in vitro. PLoS Pathog. 4 (5), e1000054. http://dx.doi.org/10.1371/journal.ppat.1000054.

van Marle, G., Dobbe, J.C., Gultyaev, A.P., Luytjes, W., Spaan, W.J., Snijder, E.J., 1999. Arterivirus discontinuous mRNA transcription is guided by base pairing between sense and antisense transcription-regulating sequences. Proc. Natl. Acad. Sci. U. S. A. 96 (21), 12056–12061.

van Vliet, A.L., Smits, S.L., Rottier, P.J., de Groot, R.J., 2002. Discontinuous and non-discontinuous subgenomic RNA transcription in a nidovirus. EMBO J. 21 (23), 6571–6580.

van der Hoeven, B., Oudshoorn, D., Koster, A.J., Snijder, E.J., Kikkert, M., Barcena, M., 2016. Biogenesis and architecture of arterivirus replication organelles. Virus Res. 220, 70–90.

Vasilakis, N., Guzman, H., Firth, C., Forrester, N.L., Widen, S.G., Wood, T.G., Rossi, S.L., Ghedin, E., Popov, V., Blasdell, K.R., Walker, P.J., Tesh, R.B., 2014. Mesoniviruses are mosquito-specific viruses with extensive geographic distribution and host range. Virol. J. 11, 97.

Wernery, U., Lau, S.K., Woo, P.C., 2016. Genomics and zoonotic infections: Middle East respiratory syndrome. Rev. Sci. Tech. 35 (1), 191–202.

Wickramasinghe, I.N., de Vries, R.P., Grone, A., de Haan, C.A., Verheije, M.H., 2011. Binding of avian coronavirus spike proteins to host factors reflects virus tropism and pathogenicity. J. Virol. 85 (17), 8903–8912.

Wood, O., Tauraso, N., Liebhaber, H., 1970. Electron microscopic study of tissue cultures infected with simian haemorrhagic fever virus. J. Gen. Virol. 7 (2), 129–136.

Zeng, C., Wu, A., Wang, Y., Xu, S., Tang, Y., Jin, X., Wang, S., Qin, L., Sun, Y., Fan, C., Snijder, E.J., Neuman, B.W., Chen, Y., Ahola, T., Guo, D., 2016. Identification and characterization of a ribose 2'-O-methyltransferase encoded by the ronivirus branch of nidovirales. J. Virol. 90 (15), 6675–6685.

Ziebuhr, J., Siddell, S.G., 1999. Processing of the human coronavirus 229E replicase polyproteins by the virus-encoded 3C-like proteinase: identification of proteolytic products and cleavage sites common to pp1a and pp1ab. J. Virol. 73 (1), 177–185.

Ziebuhr, J., Snijder, E.J., Gorbalenya, A.E., 2000. Virus-encoded proteinases and proteolytic processing in the Nidovirales. J. Gen. Virol. 81 (Pt 4), 853–879.

Zirkel, F., Kurth, A., Quan, P.L., Briese, T., Ellerbrok, H., Pauli, G., Leendertz, F.H., Lipkin, W.I., Ziebuhr, J., Drosten, C., Junglen, S., 2011. An insect nidovirus emerging from a primary tropical rainforest. mBio 2 (3). http://dx.doi.org/10.1128/mBio.00077-11. (e00077–e00011).

Zirkel, F., Roth, H., Kurth, A., Drosten, C., Ziebuhr, J., Junglen, S., 2013. Identification and characterization of genetically divergent members of the newly established family Mesoniviridae. J. Virol. 87 (11), 6346–6358.